Effect of the skimming layer on electro-osmotic — Poiseuille flows of viscoelastic fluids

J. J. Sousa[1*], A. M. Afonso[2], F. T. Pinho[3] and M. A. Alves[2]

[1]Lactogal, Direcção Engenharia Industrial, Rua Campo Alegre 830, 4150-171 Porto, Portugal, email: jeremias.sousa @lactogal.pt http://www.lactogal.pt
[2] Departamento de Engenharia Química, CEFT, Faculdade de Engenharia da Universidade do Porto, Rua Dr. Roberto Frias s/n, 4200-465 Porto, Portugal, aafonso@fe.up.pt; mmalves@fe.up.pt
[3] Departamento de Engenharia Mecânica, CEFT, Faculdade de Engenharia da Universidade do Porto, Rua Dr. Roberto Frias s/n, 4200-465 Porto, Portugal, fpinho@fe.up.pt

Abstract

An analytical solution is derived for the micro-channel flow of viscoelastic fluids by combined electro-osmosis and pressure gradient forcing. The viscoelastic fluid is described by the Phan- Thien— Tanner model with due account for the near wall layer depleted of macromolecules. This skimming layer is wider than the electric double layer and leads to an enhanced flow rate relative to that of the corresponding uniform concentration flow case. The derived solution allows a detailed investigation of the flow characteristics due to the combined effects of fluid rheology, forcing strengths ratio, skimming layer thickness and relative rheology of the two fluids.

Keywords: *electro-kinetic effects; Phan-Thien—Tanner fluid; Newtonian skimming layer; fully-developed channel flow; combined electro-osmosis Poiseuille flow.*

1 Introduction

The advent of cheap micro-fabrication techniques is promoting the widespread adoption of microfluidic flow devices by a large number of industrial applications, especially those dealing with bio-fluids, but also including new energy systems, such as fuel cell systems where there is flow through porous media and membranes. Accurate flow control in these devices requires techniques that can easily be miniaturized and an obvious candidate is electricity-related forcing taking advantage of electrokinetic phenomena. An overview of electrokinetic techniques can be found in Bruus [1].

In electroosmosis, flow of a polar fluid in a channel is forced by an external electric field applied between the inlet and outlet and acting on ions existing near the channel walls. These ions, often called counter-ions, appear spontaneously when the fluid is brought in contact with the solid wall as a consequence of the molecular attractive forces developing between the fluid molecules and the solid material. The ions nearest to the wall are immobile forming the Stern layer, the next neighbouring ions are mobile and form the diffuse layer. In this electric double layer (EDL) ions flow as a result of the streamwise electric potential, dragging the remaining fluid by viscous forces. In addition it is possible to induce flow by pressure gradient, but electrokinetic effects in micro-channels also creates spontaneous electro-osmosis in Poiseuille flows, i.e. in the absence of an imposed electric field the Poiseuille flow induces an electric potential, the so-called streaming potential [2], leading to electro-osmotic flow.

The principle of electro-osmosis was demonstrated by Reuss [3] early in the 19th century and has been subsequently developed, especially over the last 30 years. Today, there are rigorous models of electro-osmotic flows in microchannels for Newtonian fluids, such as those of Burgreen and Nakache [4] and Dutta and Beskok [5] for weak and strong surface potentials, respectively. Synthetic and bio-fluids are often made from complex molecules that impart non-linear rheological behaviour, called non-Newtonian to distinguish from the common linear stress rate-of-strain behavior of fluids made from small molecules. The first treatments of non-Newtonian effects, by Das and Chakraborty [6] and Chakraborty [7] amongst others, were limited to inelastic power law fluids, but very recently these solutions were extended to viscoelastic fluids by Afonso et al [8] and this work is a follow-up dealing with the viscoelastic flow in the presence of a depleted region of macromolecules near the walls.

In solutions of macromolecules there are additional effects that need to be accounted for in electro-osmosis due to the more complex interactive forces between the wall and the macromolecules and the obvious blockage that the wall imposes on molecular motion. As a consequence there can be wall adsorption or depletion as explained by Olivares et al [9], the latter being more common. The electro-osmotic flow of non-Newtonian power law fluids with a Newtonian skimming layer has been previously studied by Berli and Olivares [10], and here we

generalize our previous work [8] for homogeneous viscoelastic fluids to deal with the presence of a near-wall region depleted of macromolecules. The rheology of this near-wall fluid can be either Newtonian or still viscoelastic, but only the former is dealt with here.
In this paper an analytical solution is derived for the micro-channel flow of viscoelastic fluids by combined electro-osmosis and pressure gradient forcing under fully-developed conditions. The viscoelastic fluid is described by the Phan- Thien— Tanner model [11] with due account for the near wall layer depleted of macromolecules and behaving as a Newtonian fluid. This skimming layer is wider than the electric double layer and leads to an enhanced flow rate relative to that of the corresponding uniform concentration flow case. The derived solution allows a detailed investigation of the flow characteristics due to the combined effects of fluid rheology, forcing strengths ratio and the ratio between the ticknesses of the skimming layer and of the EDL.

2 Governing equations

Fig. 1 shows schematically the flow geometry and illustrates also the electro-osmosis phenomenon showing in addition the depletion layer, also called skimming layer, since it is here assumed that there are repulsive forces between the macromolecules and the wall. The nomenclature used is that of our previous work [8]. Close to the wall there is a Newtonian fluid and in the core there is the viscoelastic fluid. Both layers are subject to the electrokinetic field and the pressure gradient forcings, but as we shall see the direct impact of electro-osmosis on the PTT velocity profile is fairly weak. The layer depleted of macromolecules has a thickness (δ_L) and it is usually larger than the thickness (ξ) of the electric double layer (EDL). This is so because the thickness of the skimming layer is of the order of the radius of gyration of the macromolecules, whereas the EDL is often of the order of 10 to about 100 nm, i.e., $\xi < \delta_L$ [9]. Given this flow structure electro-osmosis is usually present essentialy inside the skimming layer and the electrokinetic effects are carried into the outer viscoelastic fluid region by viscous dragging at the interface. However, for generality the analytical solution derived here takes into account electrokinetic effects also within the viscoelastic fluid. If macromolecular depletion in the skimming layer is complete, the fluid there is the Newtonian solvent.

Regardless of whether there is a skimming layer the EDL is composed of a very thin layer of stagnant fluid densely populated with counterions, called the Stern layer, followed by a mobile layer of counterions at a smaller concentration, denoted diffuse layer [12]. The total charge in the system is neutral, i.e., there are as many ions at the wall as counterions at the EDL.

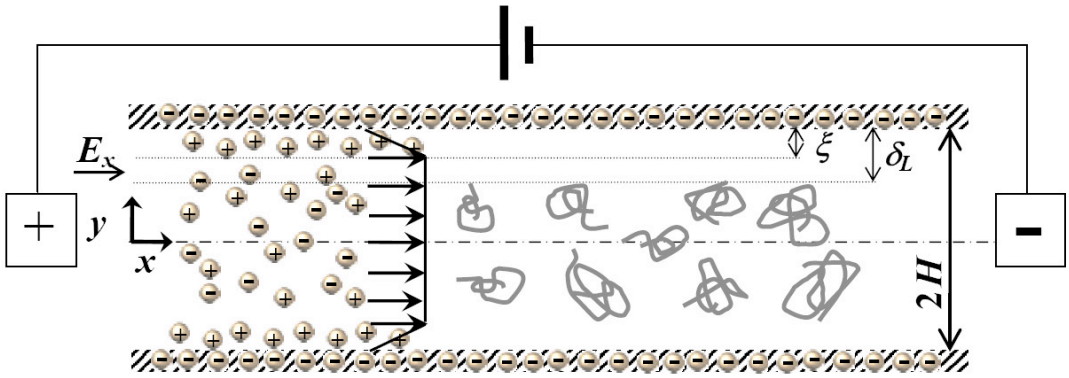

Fig. 1. Schematic representation of the electro-osmotic flow in a microchannel with a skimming layer.

As a consequence of the described fluid model, the flow governing equations to be solved for fully-developed flow are the continuity Eq. (1) and the following modified form of the Cauchy Eq. (2).

$$\nabla.\mathbf{u} = 0 \tag{1}$$

$$-\nabla p + \nabla.\boldsymbol{\tau} + \rho_e \mathbf{E} = \mathbf{0} \tag{2}$$

where **u** is the velocity vector, p is the pressure, and $\boldsymbol{\tau}$ is the fluid extra-stress tensor. In the skimming layer this extra-stress tensor describes a Newtonian fluid of viscosity η_s via Eq. (3), whereas elsewhere the fluid is described by the Phan-Thien— Tanner (PTT) model of Eq. (4). The $\rho_e\mathbf{E}$ term represents the applied external electric field (or the induced streaming potential in Poiseuille flow with electroviscous effects), where ρ_e is the net electric charge density in the fluid. If the EDL is much thinner than the skimming layer the electrical field forcing ($\rho_e\mathbf{E}$) is negligible outside the skimming layer, but for generality we keep the electro-osmotic forcing inside and outside the skimming layer and we consider always that the EDL is thinner, but not necessarily much

thinner, than the skimming layer. The electric field **E** is related to the existing potential via $\mathbf{E} = -\nabla\Phi$, where $\Phi = \psi + \phi$. ϕ is the applied streamwise potential and ψ is the potential spontaneously formed by the interaction between the walls and the fluid, which only varies in the cross-stream direction. We also consider that the electric properties of the polymer solution and Newtonian solvent are identical. As mentioned, the rheological models for the fluid inside and outside the skimming layer are expressed mathematically as

- for the solvent (layer I): $$\boldsymbol{\tau} = 2\eta_s \mathbf{D} \tag{3}$$

- for the polymeric liquid (layer II): $$f(tr\boldsymbol{\tau})\boldsymbol{\tau} + \lambda \overset{\nabla}{\boldsymbol{\tau}} = 2\eta\mathbf{D}, \tag{4}$$

where the rate of deformation tensor is $\mathbf{D} = \left(\nabla\mathbf{u} + (\nabla\mathbf{u})^{\mathrm{T}}\right)/2$, λ is the relaxation time of the polymeric fluid having a viscosity coefficient η. $\overset{\nabla}{\boldsymbol{\tau}}$ denotes the upper convected Oldroyd derivative given in Eq. (5).

$$\overset{\nabla}{\boldsymbol{\tau}} = \frac{D\boldsymbol{\tau}}{Dt} - (\nabla\mathbf{u})^{\mathrm{T}} \bullet \boldsymbol{\tau} - \boldsymbol{\tau} \bullet \nabla\mathbf{u} \tag{5}$$

The stress coefficient for the PTT model is given by its linear form [11], $f(tr\boldsymbol{\tau}) = 1 + \frac{\varepsilon\lambda}{\eta} tr\boldsymbol{\tau}$, introducing parameter ε, which is responsible for bounding the extensional viscosity.

The flow under analysis is steady, fully-developed and the electric double layers forming near each wall are sufficiently thin to be considered independent of each other. In addition, the flow geometry and conditions are symmetric, so only half the channel needs to be considered. These EDL (or Debye layers) are formed spontaneously from the contact between the dielectric walls and the polar fluid as schematically shown on the left side of Fig. 1. These conditions imply that the Nernst- Planck equations governing the ionic and induced electric potential field (ψ) distributions simplify so that in the EDL ψ is expressed by the following Poisson-Boltzmann equation [13]:

$$\nabla^2\psi = -\frac{\rho_e}{\epsilon} \tag{6}$$

where ϵ is the dielectric constant of the solution assumed constant. Following Bruus [1] the electric charge density distribution in equilibrium near a charged surface, as in this fully-developed flow geometry, is given by

$$\rho_e = -2n_0 ez \sinh\left(\frac{ez}{k_B T}\psi\right) \tag{7}$$

with n_0 representing the ionic density, e the elementary electronic charge and z the valence of the ions. k_B stands for Boltzmann constant and T is the absolute temperature.

2.1 Boundary conditions

As mentioned above, only half of the channel is considered ($0 \leq y \leq H$) given the flow symmetry, with H denoting the half-channel width. At the wall the no-slip condition applies, here for an immobile wall, and at the centreplane flow symmetry conditions apply (flow symmetry conditions are anti-symmetry of the shear stress, hence $\tau_{xy} = 0$ at $y = 0$). At the interface between the skimming layer and the bulk of the fluid a no-slip condition for velocity is valid, i.e., both fluids move at the same velocity at their interface.

Regarding the Poisson- Boltzmann equation governing the electric charge distribution, at the interface between the dielectric wall and the electrolyte fluid there is a wall potential ψ_0, also called the zeta potential, which depends on the properties of the wall and fluid. The constant potential gradient of the applied electric field in the streamwise direction ($\Delta\phi/l$, where l is the channel length) is sufficiently weak not to interfere with the induced ion distribution across the channel, i.e., $\Delta\phi/l << \psi_0/\xi$. These are the conditions of the so-called standard electrokinetic model (see [8] for further details). The potential ψ decreases very quickly with distance from the wall and even though it is not null at the skimming layer interface, it is sufficiently small to have a negligible direct influence upon the viscoelastic fluid lying outside the skimming layer, as will be seen later.

For small zeta potentials the EDL thickness is thin and for small values of $ez\psi/(k_B T)$, Eq. (7) can be linearized, i.e., $\sinh x \approx x$. This is called the Debye- Hückel approximation, which we invoke here, thus limiting the zeta potential to values smaller than 26 mV at room temperatures [4,5].

3 Analytical solution

We start by integrating the Poisson- Boltzmann equation after back-substituting Eq. (7) into Eq. (6) and considering the Debye- Hückel hypothesis of Section 2.1.

$$\frac{d^2\psi}{dy^2} = \frac{2n_0 ez \sinh\left(\frac{ez}{k_B T}\psi\right)}{\in} \rightarrow \frac{d^2\psi}{dy^2} = \frac{2n_0 e^2 z^2 \psi}{k_B T \in} \tag{8}$$

Defining the Debye- Hückel parameter (κ) as $\kappa^2 = \frac{2n_0 e^2 z^2}{k_B T \in}$, which is related to the EDL thickness by $\xi = 1/\kappa$, the integration of Eq. (8) leads to the transverse distribution of the electric potential of Eq. (9), where ψ_0 is the wall potential, also known as zeta potential.

$$\psi = \psi_0 \frac{\cosh(\kappa y)}{\cosh(\kappa H)} \tag{9}$$

The corresponding distribution of the electric charge density is obtained by back substitution in Eq. (7) and is given by $\rho_e = -\in \kappa^2 \psi_0 \frac{\cosh(\kappa y)}{\cosh(\kappa H)}$, which is positive when the wall charge is negative, as it should.

We can now integrate the momentum equation, which for the streamwise component is expressed as

$$\frac{d\tau_{xy}}{dy} = -\rho_e E + p_{,x} \rightarrow \frac{d\tau_{xy}}{dy} = -\left(-\in \kappa^2 \psi_0 \frac{\cosh(\kappa y)}{\cosh(\kappa H)}\right) E_x + p_{,x} \tag{10}$$

and its integration results in the following shear stress distribution

$$\tau_{xy} = \in \kappa \psi_0 E_x \frac{\sinh(\kappa y)}{\cosh(\kappa H)} + p_{,x} y \,. \tag{11}$$

Note that the constant of integration appearing from the integration of Eq. (10) is null due since $\tau_{xy} = 0$ at the centreplane.

To determine the velocity field, it is now necessary to consider the correct expressions for the shear stress from the corresponding rheological equations, a task performed in the next two subsections.

3.1 Skimming layer (Layer I)

Inside the skimming layer ($H - \delta_L \le y \le H$) the velocity profile is obtained from integration of Eq. (12) subject to the no-slip boundary condition at the wall ($u = 0$ at $y = H$), which results in the expression of Eq. (13) for the velocity profile. This velocity profile is written as the sum of two contributions: u_E is the velocity profile for pure electro-osmotic flow (in the absence of pressure gradient forcing) and u_P is for pure Poiseuille flow (in the absence of electro-osmosis). The two contributions are independent since the superposition principle is valid for the Newtonian fluid [8].

$$\eta_s \frac{du}{dy} = \in \kappa \psi_0 E_x \frac{\sinh(\kappa y)}{\cosh(\kappa H)} + p_{,x} y \,. \tag{12}$$

$$u_I(y) = u_{E-I}(y) + u_{P-I}(y) \text{ with} \tag{13-a}$$

$$u_{E-I}(y) = \frac{\in \psi_0 E_x}{\eta_s}\left[\frac{\cosh(\kappa y)}{\cosh(\kappa H)} - 1\right];\ u_{P-I}(y) = \frac{p_{,x}}{2\eta_s}\left(y^2 - H^2\right) \tag{13-b}$$

3.2 Outside the skimming layer (Layer II)

Outside the skimming layer ($0 \le y \le H - \delta_L$) the PTT fluid leads to a more complex expression. As in other fully-developed channel flows of the PTT fluids (cf. [8, 14]), simplification of Eqs. (4) and (5) leads to the following relationships between the velocity gradient and the two non-zero components of the extra stress tensor.

$$\frac{du}{dy} = \frac{1}{\eta}\left(1 + \frac{\varepsilon\lambda}{\eta}\tau_{xx}\right)\tau_{xy} \tag{14}$$

with $$\tau_{xx} = \frac{2\lambda}{\eta}\tau_{xy}^2 \,. \tag{15}$$

A consequence of Eqs. (11) and (15) is the transverse distribution of the normal stress for the PTT fluid given by Eq. (16), whereas inside the skimming layer the Newtonian solvent implies τ_{xx}=0 under fully-developed flow conditions.

$$\tau_{xx} = \frac{2\lambda}{\eta}\left(\in \kappa\psi_0 E_x \frac{\sinh(\kappa y)}{\cosh(\kappa H)} + p_{,x} y \right)^2 \tag{16}$$

Back-substitution of Eqs. (15) and (11) into Eq. (14) provides the differential Eq. (17) for the velocity gradient to be integrated subject to the boundary condition of equal velocities at the interface between the skimming layer and the bulk flow, i.e., at $y = H - \delta_L$, the velocity $u_{Newtonian}(H-\delta_L) = u_{PTT}(H-\delta_L)$. This integration and application of the boundary conditions leads to the velocity profile of Eq. (19), where $\bar{A} = \cosh(\kappa y)/\cosh(\kappa H)$, $\bar{B} = \sinh(\kappa y)/\sinh(\kappa H)$, $\bar{C} = 1/\cosh^2(\kappa H)$, $\bar{D} = \tanh(\kappa H)$, $\bar{E} = \cosh\left[\kappa\left(H-\delta_L\right)\right]/\cosh(\kappa H)$ and $\bar{F} = \sinh\left[\kappa\left(H-\delta_L\right)\right]/\sinh(\kappa H)$ are used for compactness.

$$\frac{du}{dy} = \frac{1}{\eta}\left\{1 + \frac{\varepsilon\lambda}{\eta}\left[\frac{2\lambda}{\eta}\left(\in \kappa\psi_0 E_x \frac{\sinh(\kappa y)}{\cosh(\kappa H)} + p_{,x} y \right)^2\right]\right\}\left(\in \kappa\psi_0 E_x \frac{\sinh(\kappa y)}{\cosh(\kappa H)} + p_{,x} y \right) \tag{17}$$

$$u_{II}(y) = u_{E-II}(y) + u_{P-II}(y) + u_{EP-II}(y) \text{ with} \tag{18-a}$$

$$u_{E-II}(y) = \in \psi_0 E_x \left\{\frac{1}{\eta}\left[\bar{A}-\bar{E}\right] + \frac{1}{\eta_s}\left[\bar{E}-1\right]\right\} + \frac{2}{3}\frac{\varepsilon\lambda^2}{\kappa}\left(\frac{\in \psi_0 \kappa E_x}{\eta}\right)^3 \left(\bar{A}-\bar{E}\right)\left(\bar{B}^2\bar{D}^2 - 2\bar{C}\right) \tag{18-b}$$

$$u_{P-II}(y) = \frac{p_{,x}}{2}\left[\frac{y^2 - \left(H-\delta_L\right)^2}{\eta} + \frac{\left(H-\delta_L\right)^2 - H^2}{\eta_s}\right] + \frac{\varepsilon\lambda^2 p_{,x}^3}{2\eta^3}\left[y^4 - \left(H-\delta_L\right)^4\right] \tag{18-c}$$

$$u_{EP-II}(y) = \frac{6\varepsilon\lambda^2 p_{,x}}{\eta\kappa^2}\left(\frac{\in \psi_0 \kappa E_x}{\eta}\right)\left\{\frac{\in \psi_0 \kappa E_x}{\eta}\left[\frac{\kappa\bar{D}}{2}\left(y\bar{A}\bar{B} - \left(H-\delta_L\right)\bar{E}\bar{F}\right) - \frac{\bar{C}}{4}\left[(\kappa y)^2 - \kappa^2\left(H-\delta_L\right)^2\right] + \frac{\left(\bar{E}^2-\bar{A}^2\right)}{4}\right]\right.$$
$$\left. + \left[\frac{p_{,x}}{\eta\kappa}\left[\bar{A}\left[(\kappa y)^2 + 2\right] - \bar{E}\left[\kappa^2\left(H-\delta_L\right)^2 + 2\right] - 2\bar{D}\left[\kappa y\bar{B} - \kappa\left(H-\delta_L\right)\bar{F}\right]\right]\right\} \tag{18-d}$$

The velocity profile outside the skimming layer has an extra contribution, in addition to the pure electro-osmotic and pure Poiseuille flow terms. The extra term (u_{EP-II}) accounts simultaneously for both effects and is non-zero only when there is simultaneous forcing by pressure gradient and electric potential, thus showing that for the PTT fluid the superposition principle no longer applies.

3.3 Nondimensional velocity profile

It is worth presenting the main equations in a normalised form. For this purpose the following quantities are introduced: $\bar{y} = y/H$ and $\bar{\kappa} = \kappa H$ are nondimensional lengths, the Helmholtz- Smoluchowski electro-osmotic velocity $u_{sh} = -\in \psi_0 E_x/\eta$ is used to normalise the velocity and the Deborah number is based on the EDL thickness and u_{sh}, $De_k = \lambda u_{sh}/\xi = \lambda\kappa u_{sh}$ as in [8]. See also this reference for other definitions of Deborah number used in the context of pure Poiseuille flows. To account for the combined forcing of pressure gradient and electro-osmosis, the non-dimensional ratio between these two forcings is given by $\Gamma = -\left(H^2/\in \psi_0\right)\left(p_{,x}/E_x\right)$. Finally, the presence of a Newtonian fluid in the skimming layer introduces the ratio of viscosity coefficients $\beta = \eta/\eta_s$ and the normalized skimming layer thickness $\bar{\delta}_L = \delta_L/H$.

Inside the skimming layer the normalised velocity profile is rewritten as

$$\frac{u_I(\bar{y})}{u_{sh}} = \left(1-\bar{A}\right)\beta - \frac{1}{2}\beta\Gamma\left(1-\bar{y}^2\right) \tag{19}$$

where the first and second terms on the right-hand-side (RHS) are the normalized u_{E-I} and u_{P-I} contributions. The normalised profile outside the skimming layer is written as

$$\frac{u_{II}(\bar{y})}{u_{sh}} = \bar{u}_{E-II}(\bar{y}) + \bar{u}_{P-II}(\bar{y}) + \bar{u}_{EP-II}(\bar{y}) \text{ with} \tag{20-a}$$

$$\bar{u}_{E-II}(\bar{y}) = \left[\bar{E} - \bar{A}\right] + \beta\left[1 - \bar{E}\right] + 2\varepsilon De_\kappa^2\left(\bar{E} - \bar{A}\right)\left(2\bar{C} - \bar{B}^2\bar{D}^2\right) \tag{20-b}$$

$$\bar{u}_{P-II}(\bar{y}) = \frac{\Gamma}{2}\left[\bar{y}^2 - \left(1-\bar{\delta}_L\right)^2\right]\left\{1 + \frac{\varepsilon De_\kappa^2\Gamma^2}{\bar{\kappa}^2}\left[\bar{y}^2 + \left(1-\bar{\delta}_L\right)^2\right]\right\} + \frac{\Gamma\beta}{2}\left[\left(1-\bar{\delta}_L\right)^2 - 1\right] \tag{20-c}$$

$$\bar{u}_{EP-II}(\bar{y}) = \frac{6\varepsilon De_\kappa^2\Gamma}{\bar{\kappa}^2}\left\{\frac{\bar{D}}{2}\left[\bar{\kappa}\bar{y}\bar{A}\bar{B} - \bar{\kappa}\left(1-\bar{\delta}_L\right)\bar{E}\bar{F}\right] - \frac{\bar{C}}{4}\left[\left(\bar{\kappa}\bar{y}\right)^2 - \bar{\kappa}^2\left(1-\bar{\delta}_L\right)^2\right] + \frac{\left(\bar{E}^2 - \bar{A}^2\right)}{4}\right.$$

$$\left. - \frac{\Gamma}{\bar{\kappa}^2}\left[\bar{A}\left[\left(\bar{\kappa}\bar{y}\right)^2 + 2\right] - \bar{E}\left[\bar{\kappa}^2\left(1-\bar{\delta}_L\right)^2 + 2\right] - 2\bar{D}\left[\bar{\kappa}\bar{y}\bar{B} - \bar{\kappa}\left(1-\bar{\delta}_L\right)\bar{F}\right]\right]\right\} \tag{20-d}$$

3.4 Nondimensional Flow Rate

Integration of the full nondimensional velocity profile gives the relationship between the flow rate and the independent variables, in particular the forcing parameter Γ, the viscosity ratio β, the EDL thickness $\bar{\kappa}$ and thickness ratio $\bar{\delta}_L$. The normalized flow rate, which is defined as $\bar{Q} = Q/\left(u_{sh}H\right)$ is given as the sum of the following five contributions,

$$\bar{Q} = \bar{Q}_{E-I} + \bar{Q}_{P-I} + \bar{Q}_{E-II} + \bar{Q}_{P-II} + \bar{Q}_{EP-II}, \tag{21}$$

which are expressed by:

$$\bar{Q}_I = \bar{Q}_{E-I} + \bar{Q}_{P-I} = 2\beta\left\{\left[\bar{\delta}_L + \frac{\bar{D}}{\bar{\kappa}}\left(\bar{F}+1\right)\right] - \frac{1}{2}\Gamma\left[\bar{\delta}_L - \frac{1}{3} + \frac{1}{3}\left(1-\bar{\delta}_L\right)^3\right]\right\} \tag{22-a}$$

$$\bar{Q}_{E-II} = 2\left(1-\bar{\delta}_L\right)\left[\beta + \bar{E}(1-\beta)\right] - \frac{2\bar{F}\bar{D}}{\bar{\kappa}} + \frac{4\varepsilon De_\kappa^2\left(1-\bar{\delta}_L\right)}{3\bar{\kappa}}\left\{2\bar{C}\left[\bar{F}\bar{D} - \bar{E}\bar{\kappa}\left(1-\bar{\delta}_L\right)\right] + \frac{\bar{F}^2\bar{D}^2}{3}\left[-\bar{F}\bar{D} + 3\bar{E}\bar{\kappa}\left(1+\bar{\delta}_L\right)\right]\right\} \tag{22-b}$$

$$\bar{Q}_{P-II} = -\Gamma\left(1-\bar{\delta}_L\right)\left\{\frac{2}{3}\left(1-\bar{\delta}_L\right)^2\left[1 + \frac{6\varepsilon De_\kappa^2}{5\bar{\kappa}^2}\Gamma^2\left(1-\bar{\delta}_L\right)^2\right] + \beta\bar{\delta}_L\left(2-\bar{\delta}_L\right)\right\} \tag{22-c}$$

$$\bar{Q}_{EP-II} = 12\varepsilon De_\kappa^2\Gamma\left(1-\bar{\delta}_L\right)^3\left\{\frac{\bar{C}}{6}\left(1-\bar{\delta}_L\right) - \frac{\bar{E}\bar{F}\bar{D}}{2\bar{\kappa}}\right\}$$

$$- \frac{12\varepsilon De_\kappa^2}{\bar{\kappa}^5}\Gamma^2\left(1-\bar{\delta}_L\right)\left\{3\bar{F}\bar{D}\left[2 + \bar{\kappa}^2\left(1-\bar{\delta}_L\right)^2\right] - \bar{\kappa}\bar{E}\left(1-\bar{\delta}_L\right)\left[6 + \bar{\kappa}^2\left(1-\bar{\delta}_L\right)^2\right]\right\} \tag{22-d}$$

4 Discussion of flow results

The above equations allow us to understand better the flow dynamics via some plots, which are analysed below. We start by looking at Fig. 2a), to pure EO flow ($\Gamma = 0$), which pertains to a situation with $\beta = 1$ Also, first we concentrate our attention to the analysis of the four Newtonian curves ($\varepsilon De_\kappa^2 = 0$) at different values of $\bar{\kappa}$, which are plotted in colours other than black for easier identification. Since $\beta = 1$ these four cases are indeed equivalent to a single Newtonian fluid. One of the effects we want to investigate in this work is that of the ratio between the thicknesses of the skiming layer and of the EDL, which is here carried out by fixing $\bar{\delta}_L$ at 0.1 and varying $\bar{\kappa}$. Since $\bar{\delta}_L > \bar{\kappa}^{-1}$, then it must be that $\bar{\delta}_L\bar{\kappa} \geq 1$. These four profiles in Fig. 2a) exhibit a large shear rate at the wall and a nearly constant plateau outside the EDL. Since the velocity is normalized by the Smoluchowski velocity, the plateau value is equal to 1 and here the effect of EDL thickness is clear from this plot.

However, a skimming layer has usually a lower viscosity and this entails $\beta > 1$. Looking for the same four cases in Fig. 2b) i.e., the four coloured curves pertaining to Newtonian fluid outside the skimming layer, this plot shows the corresponding velocity profiles for $\beta = 10$ all other quantities being identical. Direct comparison between the coloured profiles in Figs. 2a) and 2b) shows that the normalised velocities with $\beta = 10$ are higher than those for $\beta = 1$ by a factor of up to 10. This is actually a consequence of the use of the higher inner fluid

viscosity coefficient to calculate the Smoluchowski velocity scale used in the normalization. In fact, when the skimming layer is much thicker than the EDL, say $\bar{\kappa} = 100$ and $\bar{\delta}_L = 0.1$, the fluid near the wall is still the same solvent as in Fig. 2a) and the electro-osmosis acts identically, but by using a velocity scale which is ten times lower than the true Smoluchowksi velocity fictitously increases the normalized velocity. We also observe that at the skimming layer interface the velocity profile is already constant. However, as the thicknesses of the two layers approach each other the action of the EDL is felt directly inside as well as outside the skimming layer and at the layer interface the profile is not yet constant. In these cases the electro-osmosis effect reaches a lower maximum velocity and a kink is also observed at the interface, because of the sudden increase in viscosity and the concomittant sudden reduction in shear rate associated with the constant value of the shear stress. Hence, values of $u/u_{sh} < \beta^{-1}$ indicate a reduction in the true flow rate due to the higher fluid viscosity outside the skimming layer.

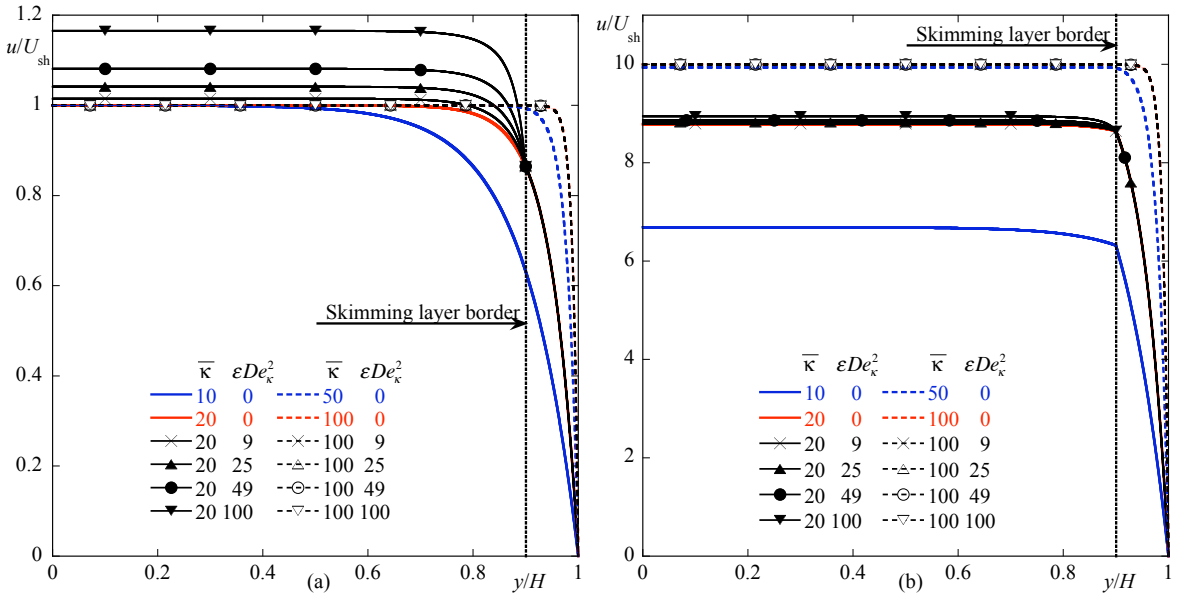

Fig. 2. Effects of $\bar{\kappa}$ and εDe_κ^2 on the profiles of normalized velocity for sPTT fluids in pure EO flow ($\Gamma = 0$) with $\bar{\delta}_L = 0.1$: (a) $\beta = 1$; (b) $\beta = 10$.

Still for pure EO flow the remaining curves (black curves) in Figs. 2a) and 2b) now analyse the effect of $\bar{\kappa}$ in combination with the effect of shear-thinning quantified by parameter εDe_κ^2 for β=1 and 10, respectively. The shear viscosity of the sPTT fluid is characterized by a Newtonian plateau at low shear rates followed by the shear-thinning effect at larger shear rates. Since in pure EO the high shear rates are found only near the wall, where the skimming layer is actually occupied by a Newtonian fluid, the fluid outside the skimming layer behaves essentially as a Newtonian fluid when $\bar{\delta}_L \bar{\kappa} >> 1$ as is clear from the collapse of the curves for $\bar{\kappa} = 100$ and in spite of the large values of εDe_κ^2. As the thickness of the skimming layer approaches the thickness of the EDL ($\bar{\delta}_L \bar{\kappa} \to 1$) then the shear-thinning becomes noticeable because at the interface the shear layer is no longer negligible and there is a sudden jump in viscosity.

Here, we must distinguish between the two situations shown in Figs. 2a) and 2b). In Fig 2b) the fluid outside the skimming layer is more viscous than the skimming layer fluid ($\beta = 10$) and on crossing the interface from the skimming layer to the bulk fluid there is a sudden increase in flow resistance, and a concomittant reduction in shear rate, so the effect of shear-thinning is fairly weak even with large values of εDe_κ^2. In Fig. 2a) there is apparently a large effect of εDe_κ^2, but the depicted situation is unrealistic. In fact, with $\beta = 1$, the zero shear rate viscosity of the sPTT fluid is identical to the viscosity of the skimming layer Newtonian fluid, meaning that at shear rates above the threshold of shear-thinning the PTT fluid will be less viscous than the Newtonian fluid. This results in the observed large effect of shear-thinning for this particular limiting case, where in reality the bulk fluid will be more viscous than the skimming fluid corresponding to β>1 and the true situation more akin

to that shown in Fig. 2b). In conclusion, for pure electroosmosis the effect of εDe_κ^2 is essentially non-existent when the EDL is much thinner than the skimming layer and fairly weak otherwise.

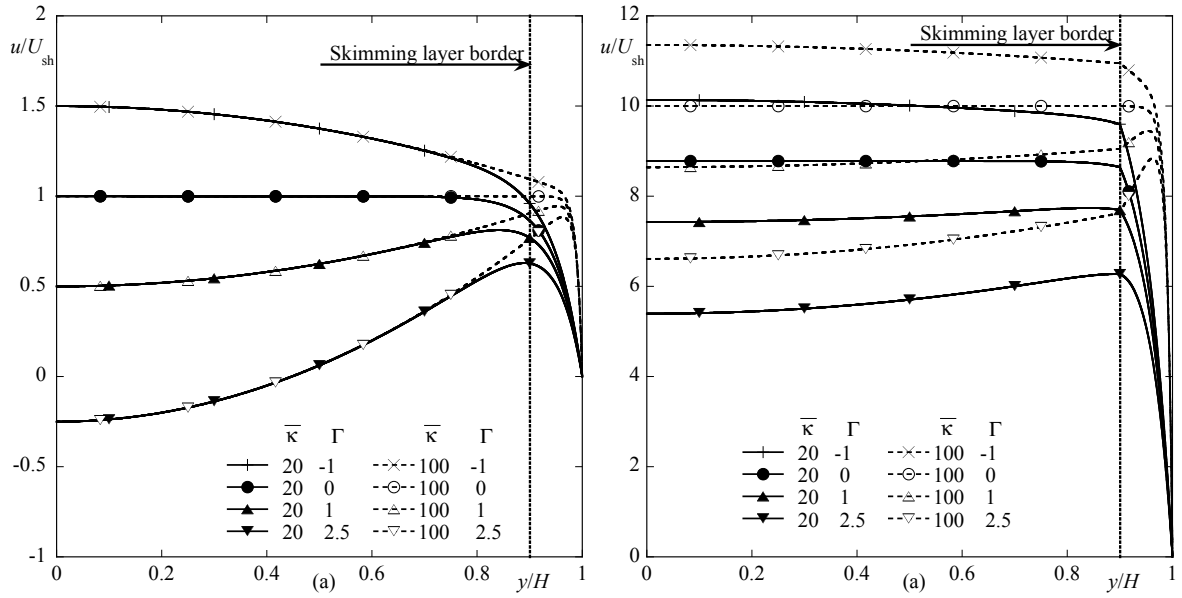

Fig. 3. Combined effect of $\bar{\kappa}$ and Γ on the profiles of normalized velocity of Newtonian fluids ($\varepsilon De_\kappa^2 = 0$) under combined forcing ($\Gamma \neq 0$) with $\bar{\delta}_L = 0.1$: (a) $\beta = 1$; (b) $\beta = 10$.

Fig. 3 plots velocity profiles for Newtonian fluids in a situation with combined forcing (pressure gradient in addition to electro-osmosis). The plots in Fig. 3a) correspond to a single fluid, since $\beta = 1$, and include both the adverse and favorable pressure gradients as well as the effect of $\bar{\kappa}$. The profiles are in agreement with those of Afonso et al [8]. Except for the EDL region the normalized profiles are identical elsewhere for the same values of all other quantities but $\bar{\kappa}$, with the profiles at higher values of $\bar{\kappa}$ showing higher velocities near the wall. As these correspond to the single fluid of Afonso et al [8], the onset of reverse flow occurs for $\Gamma = 2$, even though this curve is not shown here.

When the bulk fluid is more viscous than the fluid in the skimming layer by a factor of 10 ($\beta = 10$), the corresponding profiles are represented in Fig. 3b), all other parameters being equal. There are important qualitative differences between Figs. 3a) and 3b). Velocity profiles for different values of $\bar{\kappa}$, with all other parameters identical, now are different. The value of Γ required for reverse flow is now larger and dependent of $\bar{\kappa}$. Since forcing is no longer exclusively by a surface mechanism the stresses are larger at the skimming layer interface than for pure EO flow and consequently the kink in the velocity profile is more apparent. Only part of the differences are related to the viscosity coefficient defining the Smoluchowski velocity scale used to normalise the profile. In fact, if the Newtonian solvent viscosity is used instead, all the profiles are reduced by a factor of β, but their relative position remains the same, i.e., say for $\Gamma = 2.5$ we still do not have reverse flow . Qualitatively the surface forcing mechanism acts exclusively on the low viscosity fluid (when $\bar{\delta}_L \bar{\kappa} >> 1$) whereas the pressure forcing acts everywhere, i.e., for $\bar{\delta}_L = 0.1$ it acts upon the 81% of the total surface area occupied by the viscous fluid and on the 19% occupied by the Newtonian solvent, thus the pressure gradient needs to be stronger in order to obtain the same profile than in Fig 3a). Hence, it is clear that having a skimming layer with a less viscous fluid gives rise to different solutions than those for a single fluid. The exact quantification of this difference and whether a simple expression can be used to correct the single fluid solution of Afonso et al [8] to provide the two fluid solution is left for a subsequent more extensive investigation of the data.

Fig. 4 shows plots for the sPTT fluid to investigate the combined effects of all parameters. When $\bar{\delta}_L \bar{\kappa} >> 1$ ($\bar{\kappa} = 100$) and regardless of whether $\beta = 1$ or $\beta = 10$, the sPTT profiles are very close to the Newtonian profiles for εDe_κ^2 of up to 100. We observe a small effect for the stronger adverse pressure gradient and a similar effect is expected for larger favourable pressure gradients (not plotted for conciseness), but these are only observed if

simultaneously the value of εDe_κ^2 is quite large, because for low values of εDe_κ^2 and $|\Gamma|$ the range of shear rates outside the skimming layer are within the first Newtonian plateau of the viscoelastic fluid.

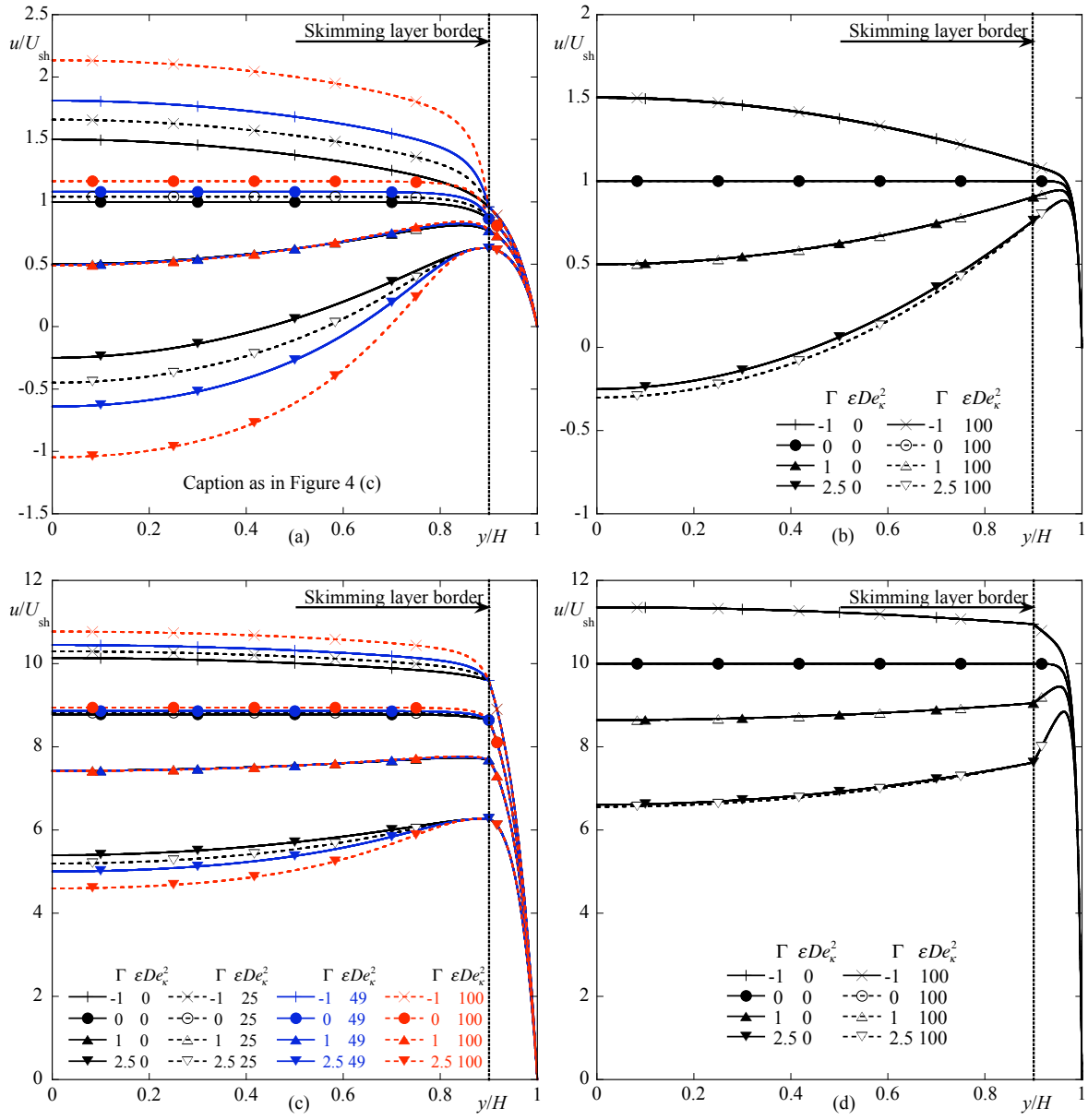

Fig. 4. Profiles of normalized velocity for sPTT fluids under combined forcing with $\bar{\delta}_L = 0.1$: (a) $\beta = 1$ and $\bar{\kappa} = 20$; (b) $\beta = 1$ and $\bar{\kappa} = 100$; (c) $\beta = 10$ and $\bar{\kappa} = 20$; (d) $\beta = 10$ and $\bar{\kappa} = 100$.

However, a small shear-thinning effect is already observed when $\bar{\delta}_L \bar{\kappa} \to 1$ ($\bar{\kappa} = 20$) and especially for lower values of β ($\beta = 1$), conditions which allow the shear rates outside the skimming layer to be in the power law region. As we mentioned before, the conditions with $\beta = 1$ are unrealistic because the bulk fluid becomes less viscous than the skimming layer fluid, but it is obvious that there is an intermediate range of conditions for which the shear-thinning characteristics of the fluid will have a non negligible impact on the flow characteristics. This corresponds roughly to $1 < \beta < 10$ and $1 < \bar{\kappa}\bar{\delta}_L < 10$, but the upper limits of these two ranges may rise the larger the value of $|\Gamma|$. Incidentally, note also from Figs. 4a) and c) that for $\Gamma = -1$ there is essentially no effect of εDe_κ^2, because the variations imposed by εDe_κ^2 and Γ cancel each other.

5 Conclusions

Solutions of macromolecules tend to migrate towards or away from the walls depending on the interactive forces at play between the wall, the solvent and the molecules, thus forming either an adsorpion or a skimming layer, respectively. When a layer depleted of molecules is formed, a possible model describing the behavior of a viscoelastic fluid is that of skimming layer near the wall with a Newtonian fluid and an outer layer away from the wall with the unmodified viscoelastic solution. An analytical solution was derived for such a generalized model and the results have shown that the flow becomes dominated by the Newtonian wall layer especially when the electric double layer ($\bar{\kappa}^{-1}$) is much thinner than the skimming layer thickness ($\bar{\delta}_L$), even for large values of εDe_κ^2 and when the viscosity of the Newtonian fluid is much lower than the zero shear rate ($\beta >> 1$).

The shear-thinning nature of the viscoelastic fluid influences the flow characteristics essentially at intermediate flow conditions, i.e., $1 < \bar{\kappa}\bar{\delta}_L < 10$ and for $1 < \beta < 10$.

Acknowledgments

The authors wish to thank funding by FCT via project PTDC/EQU-FTT/70727/2006.

References

1. H. Bruus, *Theoretical Microfluidics*, Oxford Master Series in Condensed Matter Physics, Oxford University Press, Oxford, UK, 2008.
2. P. Vainshtein and C. Gutfinger, On electroviscous effects in microchannels, *Journal of Micromechanics and Microengineering*, 12, 252-256, 2002.
3. F. F. Reuss, Sur un nouvel effet de l'électricité galvanique, *Mémoires de la Societé Impériale dês Naturalistes de Moscou*, 2, 327-337, 1809.
4. D. Burgreen and F. R. Nakache, Electrokinetic flow in ultrafine capillary slits, *J. Phys. Chem.*, 68, 1084-1091, 1964.
5. P. Dutta and A. Beskok, Analytical solution of combined electroosmotic/pressure driven flows in two-dimensional straight channels: finite Debye layer effects. *Anal. Chem.*, 73, 1979- 1986, 2001.
6. S. Das and S. Chakraborty, Analytical solutions for velocity, temperature and concentration distribution in electroosmotic microchannel flows in a non- Newtonian bio-fluid. *Anal. Chim. Acta*, 559, 15-24, 2006.
7. S. Chakraborty, Electroosmotically driven capillary transport of typical non-Newtonian biofluids in rectangular microchannels, *Anal. Chim. Acta*, 605, 175-184, 2007.
8. A. M. Afonso, M. A. Alves and F. T. Pinho, Analytical solution of mixed electro-osmotic/ pressure driven viscoelastic fluids in microchannels, *J. Non-Newt. Fluid Mech.*, 159, 50-63, 2009.
9. M. L. Olivares, L. Vera- Candiotti and C. L. A. Berli, The EOF of polymer solutions, *Electrophoresis*, 30, 921-929, 2009.
10. C. L. A. Berli and M. L. Olivares, Electrokinetic flow of non-Newtonian fluids in microchannels. *J. Colloid and Interface Science*, 320, 582-589, 2008.
11. N. Phan-Thien and R. I. Tanner, New constitutive equation derived from network theory, *J. Non-Newt. Fluid Mech.* 2, 353–365, 1977.
12. J. Lyklema, S. Rovillard and J. De Coninck, Electrokinetics: the properties of the stagnant layer unravelled. *Langmuir*, 14, 5659-5663,1998.
13. H. M. Park, J. S. Lee and T. W. Kim, Comparison of the Nernst- Planck model and the Poisson- Boltzmann model for electroosmotic flows in microchannels. *J. Colloid and Interface Science*, 315, 731-739, 2007.
14. P. J. Oliveira and F. T. Pinho, Analytical solution for fully-developed channel and pipe flow of Phan-Thien—Tanner fluids. *J. Fluid Mech.*, 387, 271- 280, 1999.